

Fabrication of Bioinspired Actuated Nanostructures with Arbitrary Geometry and Stiffness

By Boaz Pokroy, Alexander K. Epstein, Maria C. M. Persson-Gulda, and Joanna Aizenberg*

Biology is replete with examples of functional structures, whose properties are unmatched in today's man-made materials. Key features of biological structures are their dynamic nature, responsive behavior, and often multifunctionality, which all comprise the goals for the next-generation smart artificial materials. There is a growing body of information describing natural structures with sophisticated design strategies, which lend the organisms and plants superior mechanical, optical, adhesive, self-cleaning, actuation, and sensing capabilities.^[1–9] Interestingly, the common feature of these largely unrelated designs is the use of fibers and high-aspect-ratio nano- and microstructures. Nanostructures on the surface of the lotus leaf render the leaves superhydrophobic, and the droplets of water containing the collected insects and dust will roll off, and so maintain a clean leaf surface.^[1] A gecko's feet are comprised of half a million setae fibers. Each seta is tipped with ~1000 nanometer-sized spatulae. This multiscale fibrous assembly offers a unique reversible adhesion mechanism, which holds geckos to surfaces in a self-cleaning fashion.^[2,3] Complex, hierarchically structured high-aspect-ratio silica fibers in the sponge Venus's Flower Basket provide amazing fiber-optical capabilities, combined with superior mechanical properties.^[4,5] Fish and amphibians have fibrous structures (cilia) on the surfaces of their bodies connected to a hair cell at their base that detect water flow.^[6,7] Due to this sensing ability, fish can swim in narrow caves—even without the possibility of eye sight—and sense other organisms moving in their vicinity.^[6] Echinoderms cover their skin with high-aspect-ratio spines and mobile pedicellaria, which provide an effective antifouling mechanism, preventing the settlement and growth of other organisms by active movement.^[8] Pedicellaria—small claw-like extensions on the aboral surface of starfish and sea urchins—essentially exist as dense arrays of environmentally responsive biological μ -actuators.^[8]

It has been a long-standing aspiration of bioinspired materials science to understand the underlying construction principles of

biological materials and to reproduce their unique features synthetically. We asked ourselves the question of whether it is feasible to design a finely tunable, multifunctional, responsive nanostructured material that will show self-cleaning properties similar to those of a lotus leaf, will be capable of movement and reversible actuation similar to that of echinoderm spines and pedicellaria, and of sensing the force field such as fish skin. While nanostructured superhydrophobic surfaces inspired by the lotus flower and the adhesive properties of gecko feet have been mimicked with success,^[10–12] actuation/sensing at the sub-micrometer scale is still a challenging goal. Sensor arrays inspired by fish skin^[13] are still lacking key features, related to their selectivity, tunable geometry, and sensitivity. We have recently demonstrated that using a hydrogel muscle one can reversibly actuate Si nanostructures, which dynamically change their orientation in response to humidity with a response time of 60 ms.^[14] While providing a successful example of bioinspired approach to controlled actuation at the nanoscale, this hybrid design had several structural limitations, including: i) the nanostructures themselves were passive units, and their movement was induced by a hydrogel that responded to one stimulus; ii) the nanostructures were made of Si and, therefore, they had a fixed, high degree of stiffness, which restricted the deflection and required high forces; and iii) with no control over the stiffness, the extent of actuation was adjusted using Si nanoarrays with various aspect ratios, which involved a highly expensive and labor-intensive deep-etching fabrication procedure for each substrate. In the current study, we wanted to take this bioinspired design to the next level, and use a truly “materials” approach to develop a low-cost procedure for producing an arbitrarily designed actuated surface, with high-aspect-ratio nanostructures that are themselves responsive to a variety of stimuli and have a finely tuned geometry and stiffness.

A soft lithography technique was recently introduced as a low-cost alternative to conventional lithography, and has been shown to be an extremely powerful method for the high-resolution replication of microfabricated substrates in an elastomeric polymer, polydimethylsiloxane (PDMS).^[15–17] PDMS has been widely used to form polymeric arrays of micrometer-sized posts for a variety of applications, including control of cellular adhesion and wettability.^[18–20] Due to the low level of stiffness of PDMS, only limited aspect ratios were achievable, and irreversible collapse was shown to occur in high-aspect-ratio posts.^[21] We have adopted and significantly extended the soft-lithography replication method to allow the fabrication of a biomimetic array of stable, high-aspect-ratio features, which represents a critical functional requirement of biological actuated nanostructures and sensors. In our approach, PDMS is not the

[*] Prof. Dr. J. Aizenberg, Dr. B. Pokroy, A. K. Epstein
M. C. M. Persson-Gulda
School of Engineering and Applied Sciences
Harvard University
29 Oxford Street, Cambridge, MA 02138 (USA)
E-mail: jaiz@seas.harvard.edu

Prof. J. Aizenberg
Department of Chemistry and Chemical Biology
Harvard University
12 Oxford Street, Cambridge, MA 02138 (USA)

DOI: 10.1002/adma.200801432

final nanostructured material: it is used as a secondary elastomeric mold for casting the replica in the material of choice. As a result, the stability and stiffness of the replicated structures can be controlled by choosing a final material with the desired mechanical properties, and the geometry of the nanostructures can be finely tuned by applying a specific deformation of the PDMS mold.

The fabrication procedure is outlined in Figure 1. The initial high-aspect-ratio master can be either formed by standard lithographical techniques, grown bottom-up (for example, nanowires), or a biological sample. In this paper, we demonstrate our procedure by replicating arrays of Si nanoposts with a pitch a_0 (distance between the posts), a post radius r_0 , and a length l_0 (Fig. 1A). We formed a negative replica of the structure coated with an antisticking thin layer in PDMS or paraffin (Fig. 1B–E). An important requirement is that the negative replica must be able to peel off or detach easily without disrupting the fine structure of Si, so that the features are accurately replicated on a large scale (Fig. 1C). The created PDMS or paraffin mold (Fig. 1D–E) has an array of wells, into which the desired material (polymer, liquid metal, or ceramics) is cast in liquid form and cured (Fig. 1F). The mold is then either peeled off (PDMS, Fig. 1G) or heated and dissolved (paraffin) to reveal the replicated structure. Figure 1H shows an epoxy-replicated nanoarray that reproduces the original master with the nanometer-scale resolution. These surfaces exhibit superhydrophobic, self-cleaning properties, and the water droplets remain suspended on the tips of the nanoarray and roll off the surface, similar to the properties reported for the original Si masters.^[22,23]

The fabrication of nanostructures with different geometries using this one-to-one double-replication procedure would require specialized, highly expensive Si masters for each design. Moreover, the lithographic procedure allows only the generation of nanostructures oriented normal to the surface. In the case of our biological “role models,” the fibers with high aspect ratio are often oriented in different directions, rather than just standing upright,^[8] and have noncircular cross-sections.^[7] This asymmetry has important functional implications. For example, it can lead to anisotropy in the adhesive properties^[24] of gecko feet on surfaces, or to anisotropy in wettability in some man-made nanostructured surfaces.^[25] The elliptical cross-section of superficial neuromasts – structures that detect water flow on the body surface of fish and

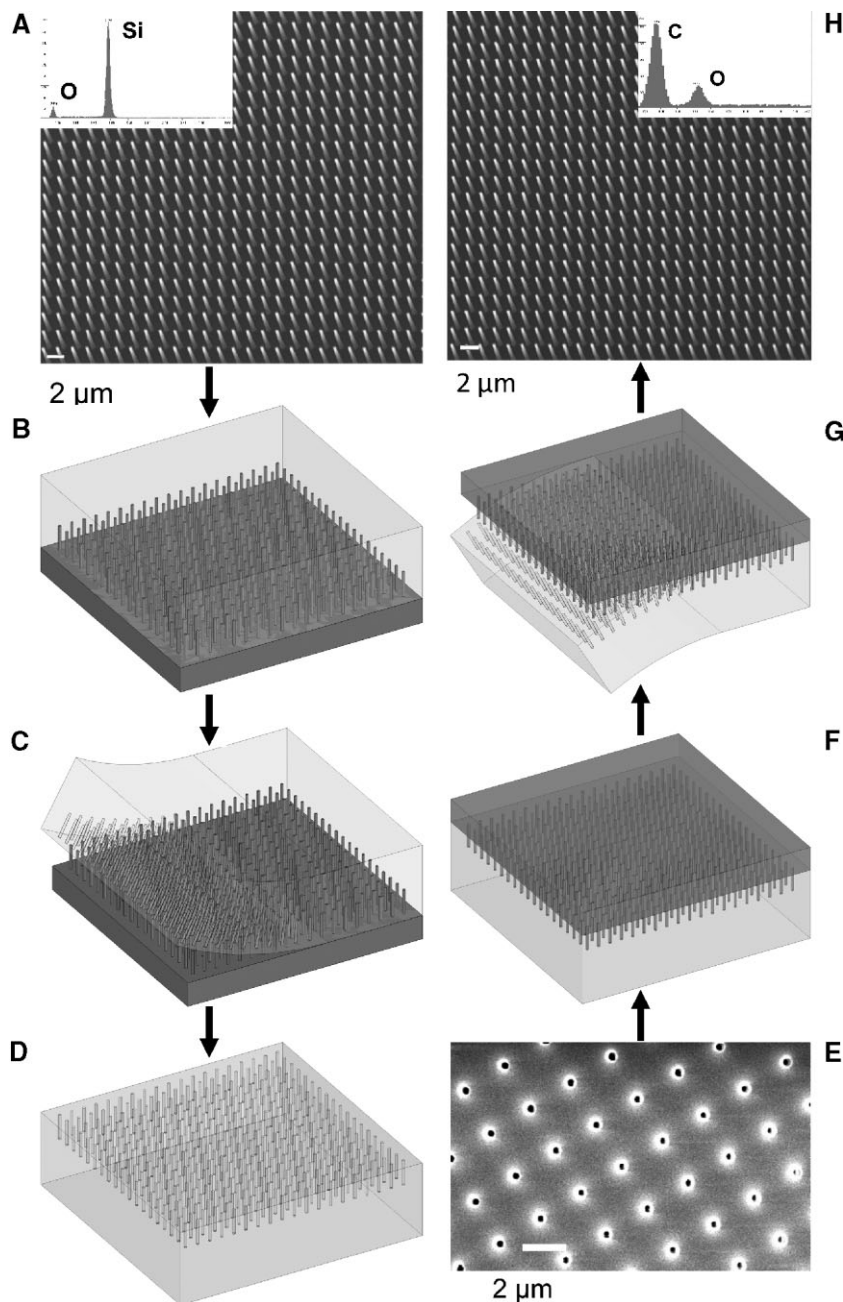


Figure 1. Two-step soft-lithography process for creating replicas of nanostructured surfaces with high-aspect-ratio features. A) SEM image of an exemplary original nanostructured surface—a silicon master bearing a square array of posts $8\ \mu\text{m}$ long with the diameter $250\ \text{nm}$ and pitch $2\ \mu\text{m}$. The oblique view is used to best visualize the structure. The insert is an EDS spectrum. B) Liquid PDMS precursor is poured onto the master, treated with an antisticking agent, and cured. C) The cured PDMS is peeled off from the master. D) The negative PDMS mold, which contains an array of high-aspect-ratio wells corresponding to the posts of the positive master, is surface-treated with an antisticking agent. E) SEM image of the PDMS mold, revealing the high-aspect-ratio wells. F) Liquid PDMS precursor (polymer, liquid metal) is poured onto the negative PDMS mold and cured. G) The PDMS mold is peeled off from the cured positive replica. H) SEM image of an exemplary nanostructured replica fabricated from epoxy resin. The insert is an EDS spectrum. The replicated structure is geometrically indistinguishable from the master shown in A).

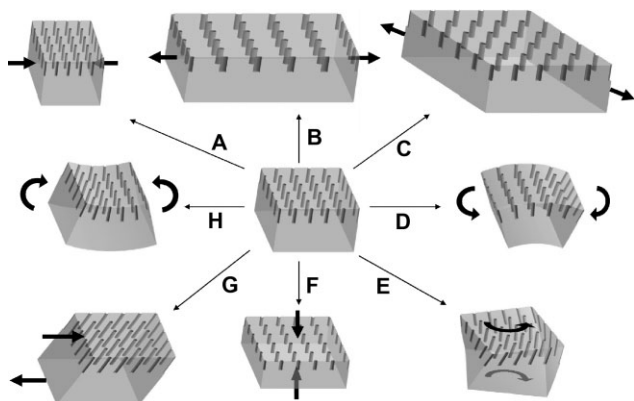


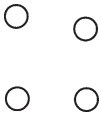
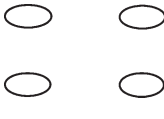
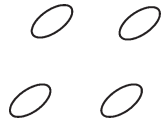
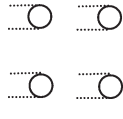
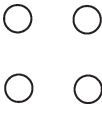
Figure 2. Schematic 3D renderings of various deformations of the PDMS mold, which allow the fabrication of arbitrary arrays of nanoposts with finely tuned geometries and nontrivial configurations. The unmodified mold (center) can be: A) compressed along the [100] direction, B) stretched along the [100] direction, C) stretched along the [110] direction, D) uniformly concavely curved, E) torsioned around the [001] axis, F) compressed along the [001] direction, G) sheared along the [100] direction, or F) uniformly curved convexly.

amphibians – provides the ability to map the direction of water flow.^[13] Motivated by these considerations, we have developed a technique by which we can easily control the geometry of the nanostructures to form both tilted and twisted posts, as well as different 2D symmetries and cross-sectional shapes, using the same original master. This is achieved by deforming the flexible negative PDMS molds before curing or solidifying the final material.

Certain example deformation types are shown in Figure 2, and the resulting changes in geometry are summarized in Table 1. By deforming the PDMS negative molds via stretching or compression in the principal directions of the 2D array of posts, we can transform the original 2D square lattice to a rectangular or rhombic lattice, and the original circular cross-sections of the nanoposts to elliptical (Table 1, Fig. 2A–C). By deforming the mold in the general $[hk0]$ direction, a parallelogram unit cell with finely tuned parameters can be formed. The amount of deformation determines both the degree of ellipticity and the unit cell of the nanoarray. Tilted structures can be formed by applying a shear deformation to the mold. The amount of shear determines the tilt angle, and the direction of the shear determines the tilt direction. The length of the posts, l_0 , can be changed by compressing the negative mold perpendicular to the 2D array (Table 1, Fig. 2F). We also have the ability to form twisted nanostructures (Fig. 2E) or curved surfaces with different radii of curvature (concave or convex), very similar to echinoderm skin (Fig. 2D and H). To ensure the fabrication of an arbitrary array of nanostructures, any combination of the deformation types can be applied. Figure 3 shows an example of an epoxy nanostructured surface that was fabricated using a compound deformation of the mold consisting of a square array of normally oriented circular wells 8 μm deep, with $a_0 = 2 \mu\text{m}$ and $r_0 = 125 \text{ nm}$. By applying 20% stretch and 12.5% shear in the [110] direction, we created a structure that exhibits tilted nanoposts with $t \cong 7^\circ$, $\theta \cong 78^\circ$, and $a \cong 2.18 \mu\text{m}$.

When engineering a functional surface bearing nanoposts with high aspect ratios, one should consider the stability of the expected structures. There are several factors that can lead to the

Table 1. Deformation-induced changes in the geometry of the replicated nanostructures [a].

Parameter	Deformation Type				
	No deformation	Stretching/compressing along [100]	Stretching/compressing [110]	Shearing along [100]	Compression along [001]
a	a_0	$1/3a_0 < a < 3a_0$	$a_0 < a < 2.1 a_0$	$a = a_0$	$a \cong a_0$
b	$b_0 = a_0$	$3a_0 > b > 1/3a_0$	$b = a$	$b = a_0$	$b = a$
θ	$\theta_0 = 90^\circ$	$\theta = \theta_0$	$12.5^\circ < \theta < 167.5^\circ$	$\theta = \theta_0$	$\theta = \theta_0$
Tilt (t)	$t_0 = 0$	$t = t_0$	$t = t_0$	$0 < t < 63.4^\circ$	$t = t_0$
Post lengths (l)	l_0	$l \cong l_0$	$l \cong l_0$	$l_0 < l \leq \sqrt{5}l_0$	$1/3l_0 < l < l_0$
Cross-section	$r_1 = r_2 = r_0$	$r_1 < r_2$	$r_1 < r_2$	$r_1 = r_2 = r_0$	$r_1 = r_2 > r_0$
2D array symmetry	Square 	Rectangular 	Rhombic 	Square 	Square 

[a] [a]The calculations were performed using the reported PDMS extensibility parameter of 300% and a Poisson's ratio $\nu = 0.5$.^[26]

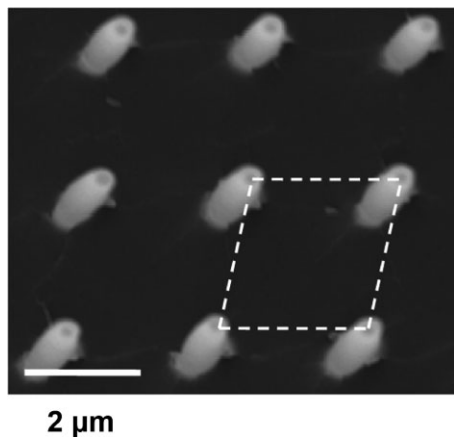


Figure 3. SEM image of an epoxy nanopost array fabricated using a compound deformation that included a 20% stretch and 12.5% shear in the [110] direction, viewed normal to the surface. The 2D array of posts displays a rhombic symmetry (unit cell highlighted). This combined deformation-mode created a structure that exhibits tilted nanoposts with $t \cong 7^\circ$, $\theta \cong 78^\circ$, and $a \cong 2.18 \mu\text{m}$.

collapse of nanoposts:^[27] collapse due to self-weight;^[28] due to adhesion forces between the posts and the base surface;^[21] and due to lateral adhesion.^[28] Calculations show that the first two are too insignificant to affect our structures; however, the importance of the second factor increases with the fabrication of the tilted nanostructures. The lateral adhesion force is the strongest of the three, and has to be taken into account. The critical aspect ratio, below which there will be no lateral collapse, is given by^[21,26]

$$\frac{l}{d} = \left(\frac{0.57E^{1/3}a^{1/2}}{\gamma_s^{1/3}d^{1/6}(1-\nu^2)^{1/12}} \right) \quad (1)$$

where d is the diameter of the posts, γ_s the surface energy, ν the Poisson ratio of the nanostructured material, and a is the pitch.

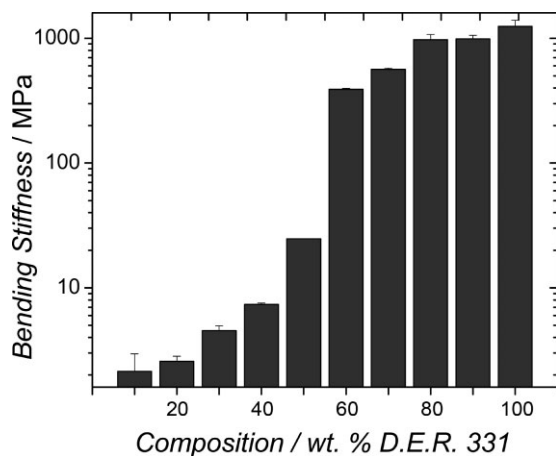


Figure 4. Histogram presenting four orders of magnitude in post flexural modulus as a function of the ratio of D. E. R. 331 (stiff epoxy resin) to D. E. R. 732 (soft epoxy resin) in weight percent. The tests were performed on a four-point flexure tester, and thus reflect pure bending conditions.

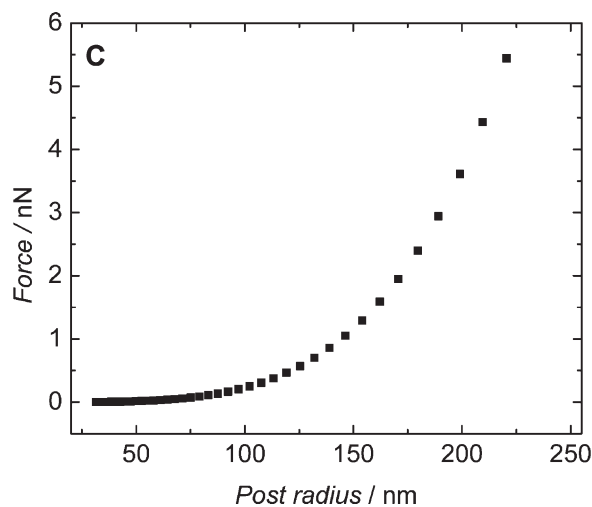
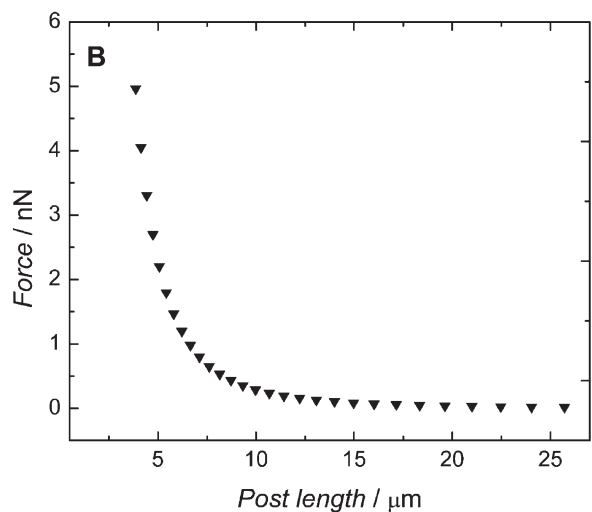
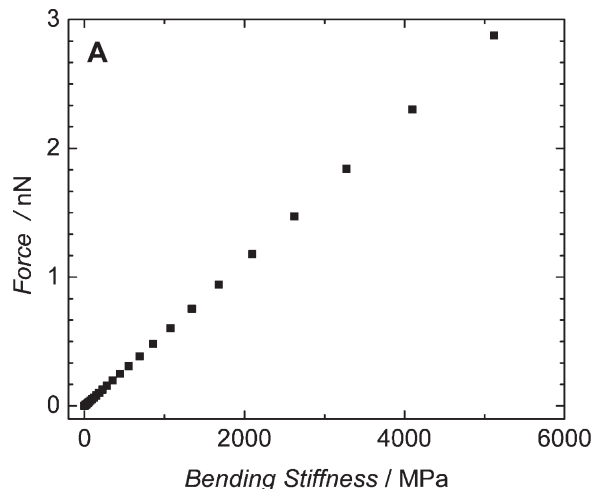


Figure 5. Mechanical characteristics of the structures, demonstrating the force applied at the tip of a post needed to bend the post to a given deflection, $Y_{1z} = 0.5 \mu\text{m}$, as a function of A) post bending modulus ($l = 8 \mu\text{m}$, $r = 125 \text{nm}$), B) post length ($r = 125 \text{nm}$, and $E = 1 \text{GPa}$), and C) post radius ($l = 8 \mu\text{m}$, $E = 1 \text{GPa}$).

An additional advantage of using the soft-lithography procedure to replicate the original master is the ability to regulate the stiffness of the resulting nanostructures. For example, the stiffness of the nanostructured array with the same geometry can vary from a few megapascal to hundreds of gigapascal, when the replicas are composed of polymers and metals/ceramics, respectively. Even more importantly, the stiffness of the array can be finely tuned by mixing two polymers that show high and low stiffness in different proportions. To demonstrate this capability, we chose to use two epoxy-based polymers: a high-viscosity resin with a post-cure higher modulus, and a low-viscosity resin with a post-cure low modulus. We were able to produce epoxy structures with a stiffness that ranges from 1 MPa to several gigaPascals, a range of four orders of magnitude (Fig. 4). Figure 4 can be then used as a calibration curve to define the recipe for a polymer mixture that will endow a nanopost array with an arbitrary, required stiffness in the megaPascal–gigaPascal range. This latter point is extremely important, as it regards the fine-tuning of the sensing/actuation capability of the nanostructures.

The mechanics of the movement of the posts is a key issue when designing functional nanostructured materials for applications in actuation/sensing. We have previously shown that when a force is applied on the beam parallel to the initial direction of the unbent post, there is a critical force below which no bending (buckling) occurs.^[14] When the force F acts along the entire post length l , perpendicular to the posts, the deflection Y_{lz} , at a given point l_z from the base, is given by^[29] $Y_{lz} = Fl_z^3/8EI$, where E is the bending modulus and I is the moment of inertia. For a post with a circular cross-section of radius r , the moment of inertia is given by the relation $I = \pi r^4/4$. To obtain an estimate for the forces needed to actuate the structures we are producing, we can use some feasible characteristic values: $E = 1$ GPa, $l = 8$ μm , $r = 125$ nm. In this case, to deflect the tip of the post by 0.5 μm , one would need a force of about 1.5 nN. If the same force F is applied only to the tip of the post, the tip will deflect 2.67 times more ($Y_{lz} = Fl_z^3/3EI$).

A bioinspired example of the application of these nanoarrays is in flow sensors. If the structures are chemically treated to be superhydrophobic, only the tips of the posts will sense the flow. However, if, alternatively, the whole structure is hydrophilic, then the force of the flow will act on the entire post. Moreover, the demonstrated unique capability of our approach to create nanostructures with elliptical cross-sections renders it possible to design a truly biomimetic sensor, which responds to an anisotropic flow field in a manner, similar to cilia in fish and amphibians.^[13] In this case, the moment of inertia in the directions of the two radii will be $I_1 = \pi r_1^3 r_2/4$ and $I_2 = \pi r_1 r_2^3/4$, and for the given force, the deflection in the direction of r_1 compared to r_2 scales as $(r_2/r_1)^2$.

To increase the sensitivity of the nanoarray, we can reduce the radius (which scales as a power of four), increase the length (scales as a power of three), and decrease the modulus (linear dependence). Plots demonstrating the force needed to bend the posts as a function of

different parameters are shown in Figure 5. As different geometrical and mechanical parameters all have an effect on the force needed to actuate the posts, it is very helpful to introduce a unified “effective stiffness” parameter, S_{effect} , to compare different cases. We chose to define this parameter as the force per unit deflection of the posts, $S_{\text{effect}} = F/Y_{lz}$. In order to compare two structures, we take the ratio of the two S_{effect} . For a circular cross-section:

$$\frac{S_{1 \text{ effect}}}{S_{2 \text{ effect}}} = \left(\frac{E_1}{E_2}\right) \left(\frac{l_2}{l_1}\right)^3 \left(\frac{r_1}{r_2}\right)^4 \quad (2)$$

This dimensionless parameter allows the direct and simple comparison of the actuation capabilities of the nanostructures.

Due to the relatively low forces needed to move the posts in our typical structures, we can observe the actuation using scanning electron microscopy (SEM, see Fig. 6A and B and Movie 1 in the Supporting Information). In this case, the actuation is probably driven by the electrostatic forces imposed by the e-beam.^[30] This movement is reversible, and can be repeated multiple times: the posts bend into the e-beam when the beam is focused on a small area, and return to their normal orientation once the e-beam is not concentrated on a small scanning area. The actuation of the array of tilted nanoposts (as in many biological systems) is shown in Figure 6C and Movie 2 in the Supporting Information. We emphasize that this is only an illustration of the ability of these posts to respond in a controlled manner to an external force.

We are currently developing bioinspired nanostructures that actuate in response to a variety of stimuli, such as magnetic, acoustic, piezoelectric, and chemical. It is noteworthy that previous efforts in actuation/sensing on the nanometer scale have used unorganized 2D arrays of high-aspect-ratio nanostructures (see for example ref. [31]). Our biological role models are often comprised of ordered arrays of spicules, ciliated cells, or

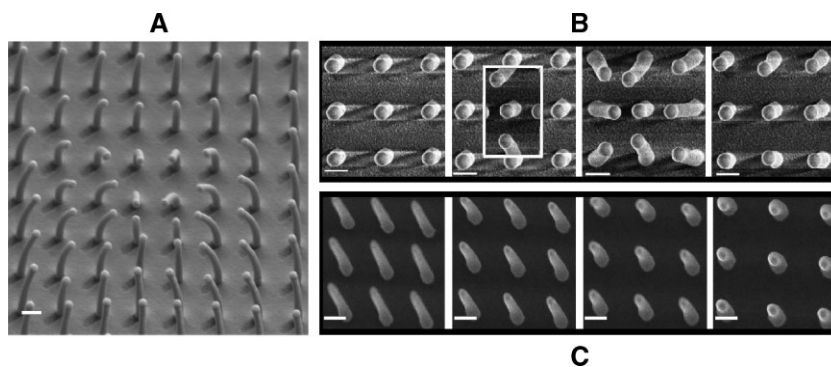


Figure 6. SEM images of the e-beam-actuated epoxy nanoposts. A) Area of posts that have been forced to bend into the center of the e-beam scanning area. This image was captured after focusing at high magnification for a short period of time, and then rapidly increasing the scanning area. The viewing angle is oblique to the surface. B) Illustration of the reversible character of the actuation process, showing snapshots from the full movie (Movie 1 in the Supporting Information). From left to right: time zero, just as the e-beam was applied; bent posts, after the e-beam was focused on the outlined area for 29.5 s, contrasted with their original condition in the frozen background; extensive post-relaxation, after the e-beam was allowed to scan a larger area again. C) Illustration of the actuation of the posts that were initially in a tilted position (produced by shearing of the PDMS mold during the epoxy-curing procedure), showing snapshots from the full movie (Movie 2 in the Supporting Information). From left to right: time zero, just as the e-beam was applied; after 1.2 s of exposure; after 2.4 s of exposure; and after 5.3 s of exposure.

pedicellaria. The ordered 2D arrays of nanostructures with high aspect ratio described here have the advantage of providing homogeneous, traceable parameters over large length scales, from sub-micrometer to centimeter scales.

In conclusion, we have shown that we can produce versatile high-aspect-ratio nanostructured surfaces inspired by the echinoderm skin, gecko foot, and superficial neuromasts in fish and amphibians. For this purpose, we have developed a soft-lithographic method that not only allows the one-to-one replication of nanostructures with high aspect ratios in a variety of materials, but also renders it possible to produce arbitrary nanostructures with cross-sectional shapes, orientations, and 2D lattices that are different from the original master. This method is the only one to our knowledge that provides such a high degree of tunability of mechanical parameters at the nanoscale and the formation of nontrivial geometries, including tilted or twisted nanostructures. The resulting bioinspired surfaces offer multifunctional characteristics that include superhydrophobic character, actuation, and sensing capabilities. We believe that these structures will find exciting applications as “smart” sensors, actuators, and other dynamic materials.

Experimental

An array of silicon nanoposts was fabricated using the Bosch process, as described elsewhere [22,32]. The silicon-nanopost arrays were treated with an antisticking agent (tridecafluoro-1,1,2,2-tetrahydrooctyl)-trichlorosilane (Gelest Inc.) by exposure in a desiccator under vacuum overnight.

Negative replicas were produced from PDMS (Dow–Sylgard 184) with a prepolymer-to-curing agent ratio of 10:1. After extensive mixing of the prepolymer and curing agent, the mixture was poured on the silicon nanopost substrate and placed in a vacuum desiccator for 1 h to eliminate all air bubbles. It was then thermally cured in an oven for 3 h at 70 °C. After cooling, the negative PDMS mold was gently peeled off the substrate. The negative PDMS mold was then cleaned extensively with ethanol, isopropanol, and acetone sequentially, dried and treated in nitrogen plasma for 1 min in a Femto Diener[®] plasma cleaner. After this surface treatment, the negative mold was placed in (tridecafluoro-1,1,2,2-tetrahydrooctyl)-trichlorosilane environment in a desiccator under vacuum overnight.

In order to produce the final replica of the master, the desired material was poured in liquid form into the negative replica wells (Fig. 1F). It is essential to ensure that this material completely fills the negative replica and solidifies inside it. In order to prevent the formation of bubbles trapped between the mold material and the original structure, a vacuum was applied over the liquid. Once the material had solidified, the negative replica was simply peeled off, leaving behind the free-standing nanostructured material. Using this method one can form replicated nanostructures from a variety of materials, such as polymers, (e.g., epoxy, PP, PE, PVA, PMMA, PDMS, various hydrogel, and shape memory polymers), metals, and alloys that have a low melting point (e.g., Ga, InBi, and Woods alloy). In this study, most of the nanostructured replicas were produced from a commercial UV-initiated one-part epoxy UVO-114[™] (Epoxy Technology). This epoxy was chosen due to the ease of use and a relatively high bending stiffness of about 1 GPa.

For the experiments involving the control of the flexural modulus of the nanostructures, two liquid epoxy resins—Dow D. E. R. 331[™], a liquid reaction product of epichlorohydrin and bisphenol A, and Dow D. E. R. 732[™], a viscosity-reducing reaction product of epichlorohydrin and polypropylene glycol—were mixed in different proportions. The mixtures were based on 10% increments of components by weight, from 10 to 100%. In all compositions, UV cross-linking initiator Cyacure UV1 6976[™] (Dow) was added to the mixture in a constant 5 wt% amount.

To produce four-point flexure-test epoxy samples, $10 \times 8 \times 62 \text{ mm}^3$ custom aluminum blocks were placed in a glass bowl; PDMS was poured and cured as described above to create molds. Each of the 11 epoxy mixtures, as well as the commercial UV-initiated one-part epoxy UVO-114 (Epoxy Technology), were sequentially pipetted into the PDMS molds flush with the tops of the wells. Each flexure sample was cured by placing molds directly under a B-100 UV lamp (UVP Blak-Ray) inside a photochemical cabinet until fully cured, which required from 20 min to several hours, depending on the composition. Mixtures with higher percentage of D. E. R. 331 required more time to cross-link.

A custom-built mechanical-test system was used to test the epoxy samples in four-point bending and to determine their flexural modulus. The system had a displacement resolution of 10 nm, controlled by a precise step motor with 100 N capacity, and a load resolution of 0.01 N. The system was set up on a pneumatic table, to shield against vibration, and was operated by a PC through LabView. The fixture's upper anvil pins were set 28 mm apart, and lower pins were spaced at 56 mm. A displacement rate of $500 \mu\text{m s}^{-1}$ and a maximum deflection of 3 mm were used for compliant samples, decreasing to 0.5–1.5 mm deflection for stiffer samples, as dictated by the step-motor maximum load. The load-deflection data were plotted into linear elastic curves, whose slopes were calculated and, along with the anvil and sample geometries, were used in the four-point bending equation to obtain the flexural moduli of the epoxy replicas.

Imaging of the nanostructures was performed using a Zeiss field-emission Ultra55 SEM. Chemical analysis was carried out in the SEM using Energy Dispersive Spectroscopy (EDS).

Acknowledgements

We would like to thank Prof. J. J. Vlassak and H. Li for the use of the four-point flexure apparatus and Prof. G. M. Whitesides and Dr. M. Reches for access to their equipment during the construction of J.A.'s laboratory. We thank Dr. A. Taylor for the fabrication of Si nanostructures. B.P. would like to extend his gratitude to the Fulbright Visiting Scholar Program for financial support. This work was partially supported by the Materials Research Science and Engineering Center (MRSEC) of the National Science Foundation under NSF Award Number DMR-0213805. Supporting Information is available online from Wiley InterScience or from the author. This article is part of a special issue on Biomaterials.

Received: May 24, 2008

Revised: July 24, 2008

Published online: November 18, 2008

- [1] W. Barthlott, C. Neinhuis, *Planta* **1997**, *202*, 1.
- [2] R. Ruibal, V. Ernst, *J. Morphol.* **1965**, *117*, 271.
- [3] K. Autumn, S. T. Hsieh, D. M. Dudek, J. Chen, C. Chitaphan, R. J. Full, *J. Exp. Biol.* **2006**, *209*, 260.
- [4] J. Aizenberg, V. C. Sundar, A. D. Yablon, J. C. Weaver, G. Chen, *Proc. Natl. Acad. Sci. U.S.A.* **2004**, *101*, 3358.
- [5] V. C. Sundar, A. D. Yablon, J. L. Grazul, M. Ilan, J. Aizenberg, *Nature* **2003**, *424*, 899.
- [6] M. J. McHenry, S. M. van Netten, *J. Exp. Biol.* **2007**, *210*, 4244.
- [7] J. Montgomery, S. Coombs, *Brain Behav. Evol.* **1992**, *40*, 209.
- [8] E. E. Ruppert, R. S. Fox, R. B. Barnes, *Invertebrate Zoology*, Brooks Cole Thomson, Belmont, CA, U.S.A. **2004**.
- [9] G. Huber, H. Mantz, R. Spolenak, K. Mecke, K. Jacobs, S. N. Gorb, E. Arzt, *Proc. Natl. Acad. Sci. U.S.A.* **2005**, *102*, 16293.
- [10] P. F. Rios, H. Dodiuk, S. Kenig, S. McCarthy, A. Dotan, *J. Adhes. Sci. Technol.* **2007**, *21*, 399.
- [11] A. K. Geim, S. V. Dubonos, I. V. Grigorieva, K. S. Novoselov, A. A. Zhukov, S. Y. Shapoval, *Nat. Mater.* **2003**, *2*, 461.
- [12] A. del Campo, C. Greiner, E. Arzt, *Langmuir* **2007**, *23*, 10235.

- [13] S. Peleshanko, M. D. Julian, M. Ornatska, M. E. McConney, M. C. LeMieux, N. Chen, C. Tucker, Y. Yang, C. Liu, J. A. C. Humphrey, V. V. Tsukruk, *Adv. Mater.* **2007**, *19*, 2903.
- [14] A. Sidorenko, T. Krupenkin, A. Taylor, P. Fratzl, J. Aizenberg, *Science* **2007**, *315*, 487.
- [15] Y. N. Xia, G. M. Whitesides, *Annu. Rev. Mater. Sci.* **1998**, *28*, 153.
- [16] Y. N. Xia, G. M. Whitesides, *Angew. Chem. Int. Ed.* **1998**, *37*, 551.
- [17] Y. N. Xia, G. M. Whitesides, *Angew. Chem. Int. Ed.* **1998**, *37*, 551.
- [18] J. L. Tan, J. Tien, D. M. Pirone, D. S. Gray, K. Bhadriraju, C. S. Chen, *Proc. Natl. Acad. Sci. U.S.A.* **2003**, *100*, 1484.
- [19] Z. J. Zheng, O. Azzaroni, F. Zhou, W. T. S. Huck, *J. Am. Chem. Soc.* **2006**, *128*, 7730.
- [20] L. Courbin, E. Denieul, E. Dressaire, M. Roper, A. Ajdari, H. A. Stone, *Nat. Mater.* **2007**, *6*, 661.
- [21] P. Roca-Cusachs, F. Rico, E. Martinez, J. Toset, R. Farre, D. Navajas, *Langmuir* **2005**, *21*, 5542.
- [22] T. N. Krupenkin, J. A. Taylor, T. M. Schneider, S. Yang, *Langmuir* **2004**, *20*, 3824.
- [23] A. Ahuja, J. A. Taylor, V. Lifton, A. A. Sidorenko, T. R. Salamon, E. J. Lobaton, P. Kolodner, T. N. Krupenkin, *Langmuir* **2008**, *24*, 9.
- [24] B. X. Zhao, N. Pesika, K. Rosenberg, Y. Tian, H. B. Zeng, P. McGuiggan, K. Autumn, J. Israelachvili, *Langmuir* **2008**, *24*, 1517.
- [25] A. D. Sommers, A. M. Jacobi, *J. Micromech. Microeng.* **2006**, *16*, 1571.
- [26] J. C. Lotters, W. Olthuis, P. H. Veltink, P. Bergveld, *J. Micromech. Microeng.* **1997**, *7*, 145.
- [27] Y. Zhang, C. W. Lo, J. A. Taylor, S. Yang, *Langmuir* **2006**, *22*, 8595.
- [28] C. Y. Hui, A. Jagota, Y. Y. Lin, E. J. Kramer, *Langmuir* **2002**, *18*, 1394.
- [29] A. R. Ragab, S. E. A. Bayoumi, *Engineering Solid Mechanics: Fundamentals and Applications*, CRC Press, Boca Raton, FL, U.S.A **1998**, p. 944.
- [30] The mechanism of the actuation under e-beam will be reported elsewhere.
- [31] B. A. Evans, A. R. Shields, R. L. Carroll, S. Washburn, M. R. Falvo, R. Superfine, *Nano Lett.* **2007**, *7*, 1428.
- [32] S. A. McAuley, H. Ashraf, L. Atabo, A. Chambers, S. Hall, J. Hopkins, G. Nicholls, *J. Phys. D: Appl. Phys.* **2001**, *34*, 2769.